

# Histopathological changes of synovial tissue in rheumatoid arthritis patients treated with TNF- $\alpha$ inhibitors or IL-6 inhibitors

Y. Takashima<sup>1</sup>, S. Hayashi<sup>1</sup>, T. Maeda<sup>1</sup>, K. Fukuda<sup>2</sup>, Y. Onoi<sup>1</sup>,  
S. Tachibana<sup>1</sup>, K. Ikuta<sup>1</sup>, K. Anjiki<sup>1</sup>, M. Fujita<sup>1</sup>, K. Kikuchi<sup>1</sup>,  
T. Kamenaga<sup>1</sup>, R. Kuroda<sup>1</sup>, T. Matsubara<sup>2</sup>

<sup>1</sup>Department of Orthopaedic Surgery, Kobe University Graduate School of Medicine, Kobe, Japan;

<sup>2</sup>Department of Orthopaedic Surgery, Matsubara Mayflower Hospital, Kato, Japan.

---

## Abstract

### Objective

To investigate the cell types that undergo apoptosis in TNF- $\alpha$  inhibitor (TNFI)- and IL-6 inhibitor (IL-6I)-treated synovia of RA patients, and to observe and compare histological changes in them.

---

### Methods

Synovial tissue was collected during total knee arthroplasty from 20 RA patients who were divided into three groups based on RA treatment received: conventional synthetic disease-modifying anti-rheumatic drugs (csDMARDs, control group), TNFI, or IL-6I. Tissue samples were subjected to haematoxylin and eosin staining, terminal deoxynucleotidyl transferase fluorescein-deoxyuridine triphosphate nick end labelling (TUNEL), immuno-histochemistry (IHC) and immunofluorescence staining for, respectively, histopathological assessment, apoptosis detection and IHC evaluation and scoring.

---

### Results

TUNEL-positive cells were detected surrounding the discoid fibrosis unique to the TNFI group, while those in the IL-6I group were distributed widely, especially surrounding the blood vessels. IHC revealed that in TNFI-treated tissue, CD86- and CD80-positive cells were detected only in the lining and sublining layer, while CD163- and CD206-positive cells were detected more broadly; in the IL-6I-treated tissue, all four were detected widely but their levels were lower than in the control group. Immunofluorescence also revealed macrophages mainly were the apoptotic cells in the lining and sublining layers of TNFI group. TUNEL Expression levels of CD20- and CD3-positive cells were remarkably lower in the IL-6I group, compared with the control and TNFI groups.

---

### Conclusion

TNFIs and IL-6Is target different action sites and synovial cell types, resulting in histopathological features of synovium distinct from one another.

---

### Key words

rheumatoid arthritis, tumour necrosis factor inhibitors, interleukins, fibrosis, synovium

Yoshinori Takashima, MD  
 Shinya Hayashi, MD, PhD  
 Toshihisa Maeda, MD, PhD  
 Koji Fukuda, MD, PhD  
 Yuma Onoi, MD  
 Shotaro Tachibana, MD  
 Kemmei Ikuta, MD  
 Kensuke Anjiki, MD  
 Masahiro Fujita, MD  
 Kenichi Kikuchi, MD  
 Tomoyuki Kamenaga, MD, PhD  
 Ryosuke Kuroda, MD, PhD  
 Tsukasa Matsubara, MD, PhD

Please address correspondence to:  
 Shinya Hayashi,  
 Department of Orthopaedic Surgery,  
 Kobe University Graduate School  
 of Medicine, 7-5-1 Kusunoki-cho,  
 Chuo-ku, Kobe, 650-0017 Japan.  
 E-mail: s11793290@yahoo.co.jp

Received on August 18, 2021; accepted  
 in revised form on December 3, 2021.

© Copyright CLINICAL AND  
 EXPERIMENTAL RHEUMATOLOGY 2022.

## Introduction

Rheumatoid arthritis (RA) is a chronic inflammatory disease that results in joint structure destruction characterised by synovial tissue hyperplasia (1, 2). The pro-inflammatory cytokines TNF- $\alpha$  and IL-6 play crucial roles in the pathogenesis of RA synovitis. TNF- $\alpha$  and IL-6 inhibitors (TNFIs and IL-6Is, respectively) have revolutionised RA treatment by achieving remission or low disease activity in patients who demonstrate inadequate responses to conventional synthetic disease-modifying anti-rheumatic drugs (csDMARDs) (3-6). TNFIs act directly on synovial cells, inducing apoptosis in TNF-producing cells, suppressing cell proliferation and inflammatory cell infiltration, and neutralising TNF- $\alpha$  (7, 8). On the other hand, IL-6Is function *in vitro* by blocking the IL-6-mediated signalling pathway via binding to both membrane-bound IL-6 receptors (IL-6Rs) and soluble IL-6Rs (9) and by suppressing angiogenesis in RA fibroblast-like synovial (FLS) cells (10). Synovial membranes of RA patients treated with TNFIs have exhibited histopathological intima (lining) changes and subintima (sublining) vasculature obstruction and degeneration (11), while those treated with IL-6Is have exhibited reduced angiogenesis and subintima degeneration (12). Because synovial histopathology in the intima and subintima can reflect disease activity (13, 14), investigation of histopathological changes in RA patient synovial tissue provides an effective method of determining TNFI and IL-6I action sites and therapeutic targets. Yet, the nature and cause of these histopathological changes, and the cell types involved, have not been investigated in detail. The purpose of this study was to observe and compare the histological characteristic changes, and investigate the cell types that undergo apoptosis, in TNFI- and IL-6I-treated synovial tissue.

## Methods

### *Patients and tissue samples*

This prospective cohort study consisted of 20 female patients diagnosed with RA, as per the diagnostic criteria of the 2010 American College of Rheumatol-

ogy/European League Against Rheumatism (ACR/EULAR) (15, 16). Patients were divided into three groups based on the following RA treatments received for at least 12 months prior to surgery: conventional synthetic disease-modifying anti-rheumatic drugs (csDMARDs; control group; n=8), TNFIs (TNFI group; n=7), and humanised anti-IL-6 receptor monoclonal antibody (IL-6I group, n=5). The control group included six patients treated with MTX, one with iguratimod, and one with salazosulfapyridine. The TNFI group included two patients treated with 6 mg/kg infliximab every 8 weeks, one patient treated with 40 mg adalimumab every 2 weeks, two patients treated with 50 mg golimumab every 4 weeks, and two patients treated with 50 mg etanercept every week. All five patients in the IL-6I group received 8 mg/kg tocilizumab every 4 weeks. Patient age, disease duration, levels of serum c-reactive protein (CRP), rheumatoid factor (RF), and matrix metalloproteinase (MMP-3), as well as erythrocyte sedimentation rate (ESR) and disease activity score-CRP (DAS28-CRP), were investigated (Table I). Patients with osteoarthritis, non-RA autoimmune diseases, and congenital diseases were excluded from this study. Synovial tissues were collected from each patient during total knee arthroplasty conducted at the Matsubara Mayflower Hospital between November 2017 and March 2021. The collected tissues were placed into the Tissue-Tek ornithine carbamyl transferase compound (Miles, Elkhart, IN), flash-frozen in liquid nitrogen, and stored at -80°C.

### *Ethics*

All samples were collected in accordance with the ethical principles of the World Medical Association Declaration of Helsinki Ethical Principles for Medical Research Involving Human Subjects. The Kobe University institutional review board approved this study (no. B190219), and informed consent was obtained from all patients.

### *Histology*

The cryosections of patient synovial tissues, 8  $\mu$ m thick, were mounted on silane-coated glass slides (Dako Japan,

Competing interests: none declared.

**Table I.** Patient demographics and disease profiles

	Control group (n=8)	95% CI	TNFI group (n=7)	95% CI	IL-6I group (n=5)	95% CI	p-value
Age (y old)	68.9	60.1–77.7	66.3	64.1–68.5	66.0	63.3–71.2	p=0.798
Disease duration (y)	12.9	4.15–21.6	18.0	11.2–24.8	18.0	12.7–23.3	p=0.415
Serum CRP (mg/dl)	0.84	0.06–1.6	0.56	-0.21–1.33	0.15	-0.16–0.46	p=0.331
ESR (mm/h)	45.1	28.2–62.1	45.2	5.77–84.8	21.2	1.9–40.5	p=0.314
RF (IU/ml)	61	13.3–108.7	49.0	10.9–87.1	96.0	46.2–145.8	p=0.268
MMP-3 (ng/ml)	192	4.69–379	75.5	21.4–129	193	44.2–429.6	p=0.382
DAS28-CRP	2.85	2.44–3.26	2.56	2.00–3.13	2.10	1.70–2.50	p=0.06

TNFI: TNF inhibitor; IL-6I: IL-6 inhibitor; DAS 28-CRP: Disease Activity Score.

Tokyo, Japan) and fixed in freshly prepared 4% paraformaldehyde buffered with 0.1 mol/l sodium phosphate (pH 7.4) at 23–27°C for 30 min. The cryosections were then stained with hematoxylin (Muto Pure Chemicals, Tokyo, Japan) and eosin (Fujifilm, Tokyo, Japan), and the histopathological parameters of each sample were assessed using light microscopy by two observers blinded to patient identities and dates. To detect the evidence of apoptosis, a terminal deoxynucleotidyl transferase fluorescein-deoxyuridine triphosphate nick end labelling (TUNEL) assay was performed using an *in situ* apoptosis detection kit (Takara, Otsu-city, Shiga, Japan) according to the manufacturer's instructions (17). Briefly, endogenous peroxidase was inactivated using 0.3% H<sub>2</sub>O<sub>2</sub> at 23–27°C for 15 min and sections were permeabilised using the permeabilisation buffer at 4°C for 5 min. Next, to label DNA 3'-OH ends with fluorescein, sections were incubated with TdT and fluorescein-dUTP at 37°C for 90 min in a dark humidified chamber. The sections were then washed three times with PBS, incubated with an anti-FITC-horseradish peroxidase (FITC-HRP) conjugate at 37°C for 30 min, washed three times with PBS, developed with 3,3'-diaminobenzidine (DAB, Nichirei Biosciences, Tokyo, Japan), and stained at 23–27°C for 5 min. The specimens were then washed three times with distilled water, counterstained with 3% methyl green for 10 min, and examined using an optical microscope.

**Immunohistochemistry**

Synovial tissue sections were probed with 1:50 dilutions of the following antibodies at 4°C overnight: mouse

monoclonal anti-CD20 (L26, Nichirei Biosciences) and rabbit polyclonal anti-CD3 (Nichirei Biosciences) to detect B and T lymphocytes, respectively; anti-CD80 (Abcam, Cambridge, UK) and anti-CD86 (Abcam, Cambridge) to detect M1 macrophages; anti-CD163 (Abcam) and anti-CD206 (Abcam) to detect M2 macrophages. Sections were subsequently incubated with peroxidase-labeled anti-rabbit or anti-mouse IgG (Histofine Simple Stain MAX PO, Nichirei Biosciences) antibody at 23–27°C for 1 h, developed using peroxidase substrate DAB for 5 min, and examined under an optical microscope. Haematoxylin was subsequently used as a counterstain. For semiquantitative analysis of synovial tissue immunohistology, the sections were evaluated using immunohistochemistry (IH) scores (18) of 0 to 5, based on a 0–100 mm visual analogue scale (VAS, expressed as % mm) with the following ranges: grade 0, [0%]; grade 1, (0%, 5%]; grade 2, (5%, 20%]; grade 3, (20%, 40%]; grade 4, (40%, 60%]; grade 5 (60%, 100%]. The IH score of each sample was assessed under 200× magnification, based on the total IH grade of the superficial, interstitial, and perivascular layers. The tertiary lymphoid structures (TLS), the characteristic histological changes of T and B lymphocytes in the RA synovium, were also assessed. For the semiquantitative analysis of TLS, anti-CD3- and anti-CD20-stained sections were evaluated under 40× magnification using the grading score described by Manzo *et al.* (19). The TLS were counted and graded from 0–3 by size with slight modification, as follows: the structure size was assessed by counting the number of cells in a radi-

us starting from an estimated centre of the aggregate. The TLS size was then classified as grade 0 (no cells), grade 1 (1–5 cells in the radius), grade 2 (5–10 cells in the radius), or grade 3 (10 or more cells in the radius).

**Immunofluorescence**

Immunofluorescence was performed to evaluate the cell types undergoing apoptosis. To detect macrophages, we used F4/80 antibody that recognises a murine macrophage-restricted cell surface glycoprotein. Briefly, sections were incubated with primary rabbit polyclonal anti-F4/80 antibody (Affinity, USA; 1:100 dilution) for 3 h at 37°C, and then with TdT and fluorescein-dUTP using an *in situ* apoptosis detection kit (Takara). Next, sections were incubated for 1 h at 23–27°C with Alexa Fluor® 568-conjugated (Thermo Fisher Scientific) and an anti-FITC-HRP-conjugated secondary antibodies, and then counterstained with 4',6-diamidino-2-phenylindole (DAPI) (Thermo Fisher Scientific, Waltham, MA, USA) to visualise DNA. Fluorescent images of TUNEL (excitation/emission: 470 nm/495 nm), F4/80 (560 nm/585 nm), and DAPI (360 nm/400 nm) were obtained using the BZ-X700 microscope. The number of positive cells was counted in five random high-power fields (200×) using the ImageJ software (<https://imagej.nih.gov/ij/>). The percentage of TUNEL-positive cells relative to the total number of DAPI-positive cells was calculated.

**Statistical analysis**

Histological assessment, IH scoring, and the grading scoring measurements were performed twice by a primary examiner and once by a secondary examiner. Cohen's kappa coefficient was calculated with a 95% CI for both inter- and intra-observer reliability in categorical variables. The degrees of reliability were used as previously described (20, 21). The kappa value of intra-observer reliability was calculated between the mean of the primary measurements and the secondary measurement of each histological features. The kappa value of inter-observer reliability was calculated between the mean of the investigator's

**Table II.** Histopathological feature summary.

	Control group (n=8)	TNFI group (n=7)	IL-6I group (n=5)	p-value	Intra-observer reliability	Inter-observer reliability
					κ -value	κ -value
Discoid fibrosis	0	7*	0	p<0.01	κ=0.783	κ=0.762
Changes in surface synovial cells						
Pyknosis	3	1	0	p=0.232	κ=0.688	κ=0.828
Hydropic degeneration	1	5*	1	p=0.042	κ=0.783	κ=0.783
Vacuolation	1	5*	1	p=0.042	κ=0.780	κ=0.894
Sublining layer degeneration, including giant cell formation	3	4	1	p=0.425	κ=0.898	κ=0.792
Sublining layer vasculature contraction or obstruction	2*	6	5	p=0.008	κ=0.780	κ=0.794
Sublining layer vasculature congestion or dilatation	4	2	1	p=0.493	κ=0.886	κ=0.894
Extensive scarring	2	4	5*	p=0.03	κ=0.773	κ=0.615
Lining layer degeneration with sublining perivascular fibrosis	2	4	5*	p=0.03	κ=0.900	κ=0.798
Lymphocyte infiltration decline	3*	6	5	p=0.03	κ=1.00	κ=0.886
Pannus formation	4*	0	0	p=0.024	κ=0.828	κ=1.00

TNFI: TNF inhibitor; IL-6I: IL-6 inhibitor.

\*significant difference between the three groups.

measurements and another investigator's measurements of each histological properties. Statistical analysis was

performed using the statistical software package SPSS 16.0 (SPSS Inc., Chicago, IL, USA). All values are expressed

as mean (95% CI). The patient backgrounds among the control, TNFI, and IL-6I groups passed the Kolmogorov-Smirnov normality test, fit the normality curve, and were analysed using one-way analysis of variance (ANOVA) and Tukey's *post-hoc* test. Categorical variables, including histological features and continuous variables, such as IH scores and the grading score of TLS, were analysed among control, TNFI, and IL-6I groups using Fisher's exact test and Kruskal-Wallis test, respectively. Statistical significance was set at  $p<0.05$ .

**Results**

The histopathological parameters of the synovial tissues from each group are summarised in Table II. The HE staining of the control group tissue showed the hyperplasia of the lining layer, infiltration of inflammatory cells, including lymphocytes, diffuse villous oedema, pannus formation, and increased neo-

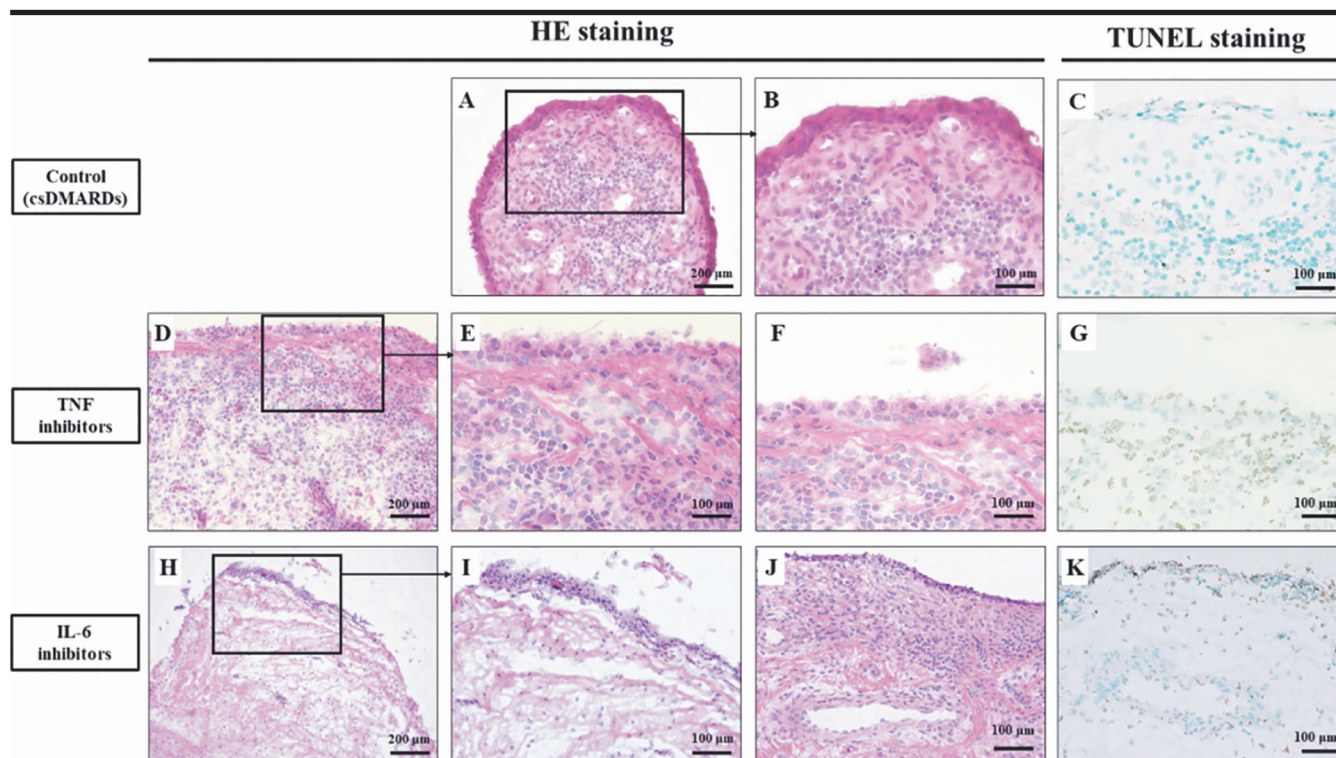


**Fig. 1.** HE and TUNEL staining of knee joint synovium.

Comparison of the histopathological findings and synovial cell apoptosis among the control, TNFI group and IL-6I groups.

**A-C:** The lining layer hyperplasia, inflammatory cell infiltration and a low number of TUNEL-positive cells are exhibited in the control group.

**D-G:** The discoid fibrosis and a greater number of TUNEL-positive cells surrounding the discoid fibrosis are exhibited in the TNFI group.

**H-K:** The marked degeneration, decreases in lymphocyte infiltration and neovascularisation and a greater number of TUNEL-positive cells surrounding the blood vessels are exhibited in the IL-6II group.

HE: haematoxylin and eosin; TNFI: TNF inhibitor; IL-6I: IL-6 inhibitor; TUNEL: TdT-mediated non-radioactive fluorescein-deoxyuridine triphosphate nick end labelling.

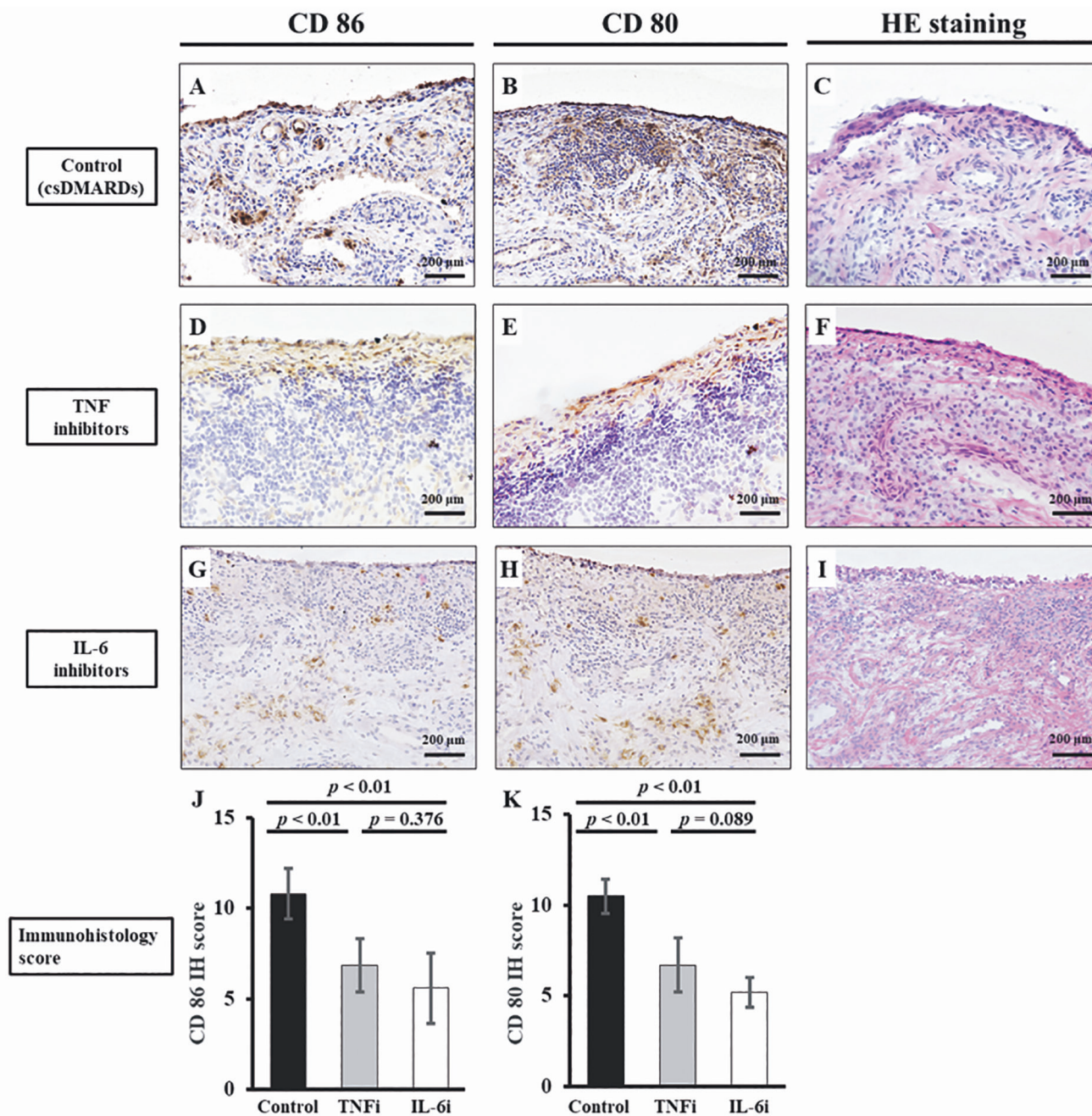


**Fig. 2.** Immunohistochemistry staining and score of CD86 and CD80 for M1 macrophage detection in knee joint synovium. A-C: In the control group, the CD86- and CD80-positive cells are widely distributed. D-F: In the TNFI group, the CD86- and CD80-positive cells are detected only in the lining and sublining layer. G-I: In the IL-6I group, CD86- and CD80-positive cells are also widely distributed, but with a lower overall number than in the control group. J-K: The CD86 and CD80 IH scores of the TNFI and the IL-6I group are significantly lower those of the control group. Kruskal-Wallis test *post-hoc* test for multiple comparisons of samples were used. CD: cluster of differentiation; TNFI: TNF inhibitor; IL-6I: IL-6 inhibitor.

vascularisation (Fig. 1A-B). Only a small number of TUNEL-positive cells was detected in the lining, sublining, and deep lining layers of the control group (Fig. 1B-C). The histopathological evaluation of the TNFI tissues demonstrated the improvement of the multi-layered synovial cells, discoid fibrosis, hydropic degeneration, vacu-

olation, and small vasculature sclerosis (Fig. 1D-E). A higher number of TUNEL-positive cells was observed in the TNFI group, particularly surrounding the discoid fibrosis (Fig. 1F-G). The IL-6I group demonstrated marked degeneration in the sublining and deep lining layers, with decreased lymphocyte infiltration and neovascularisation

(Fig. 1H-I). Furthermore, in the IL-6I group, an increased number of diffused TUNEL-positive cells was observed throughout the sublining and deep lining, particularly around the blood vessels (Fig. 1J-K). Pannus formation was observed only in the control group, while sublining vasculature contraction or obstruction

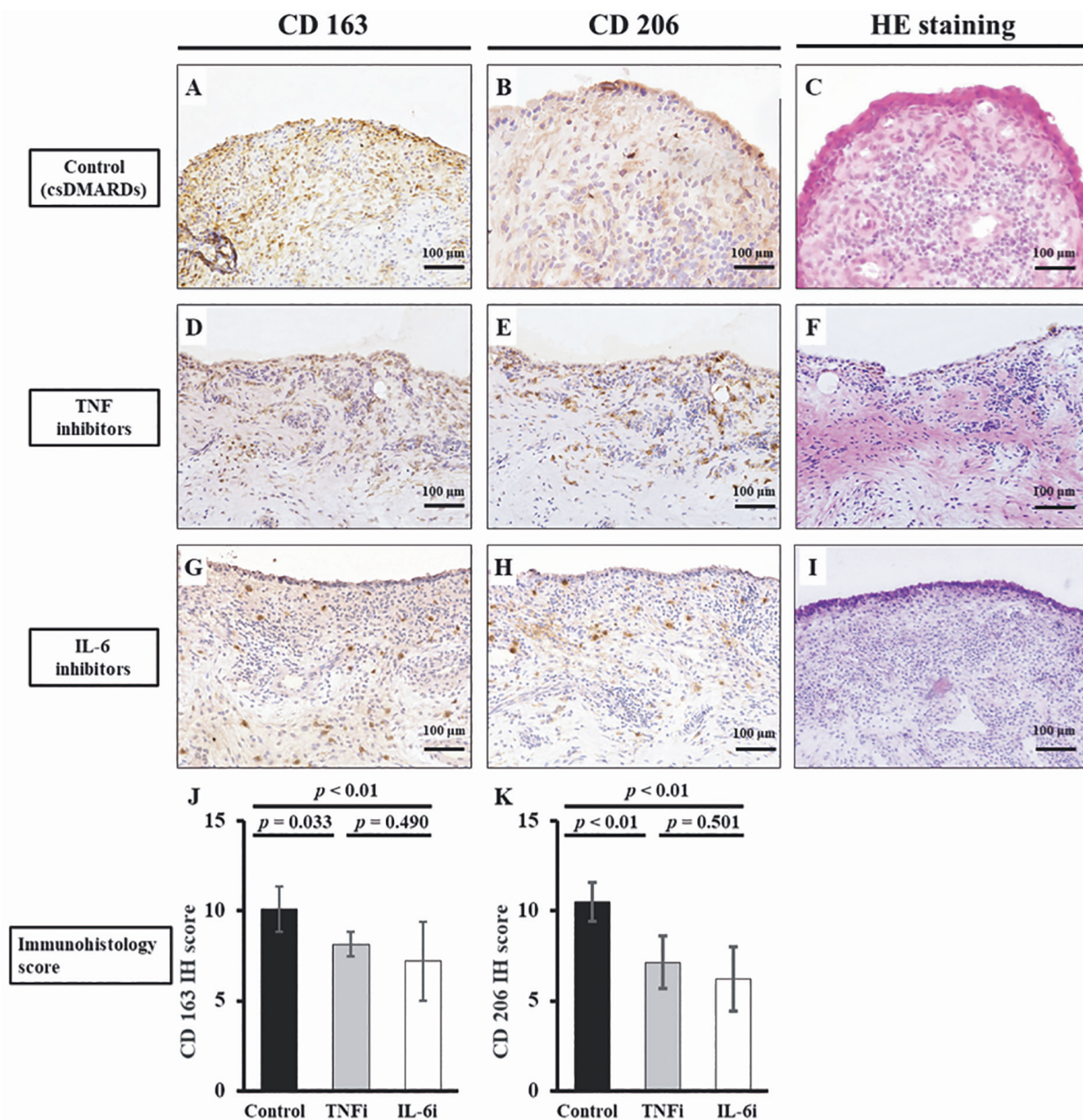


**Fig. 3.** Immunohistochemistry staining and score of CD163 and CD206 for M2 macrophage detection in knee joint synovium. In all groups, the expression of CD163- and CD206-positive cells is widely distributed. **D-I:** The TNFi and IL-6I groups exhibit lower expression of CD163- and CD206-positive cells than the control group. **J-K:** The CD163 and CD206 IH scores of the TNFi and IL-6I groups are significantly lower than those of the control group. Kruskal-Wallis test *post-hoc* test for multiple comparisons of samples were used. CD: cluster of differentiation; TNFi: TNF inhibitor; IL-6I: IL-6 inhibitor.

and decreased lymphocyte infiltration were noted in the control group less frequently than in TNFi and IL-6I groups. The TNFi group showed a significantly higher prevalence of hydropic degeneration and vacuolation compared to control and IL-6I groups, and its most common histopathological

finding – discoid fibrosis in the lining and sublining layer – was unique to this group. Lining layer degeneration, sublining layer perivascular fibrosis, and extensive scarring were observed more frequently in the IL-6I group than in control and TNFi groups. Immunohistochemistry showed that

CD86- and CD80-positive cells were widely distributed in control (Fig. 2A-C) and IL-6I (Fig. 2G-I) groups, with lower expression levels in the latter; however, these cells could only be detected in the lining and sublining layer of the TNFi group (Fig. 2D-F). CD163- and CD206-positive cells

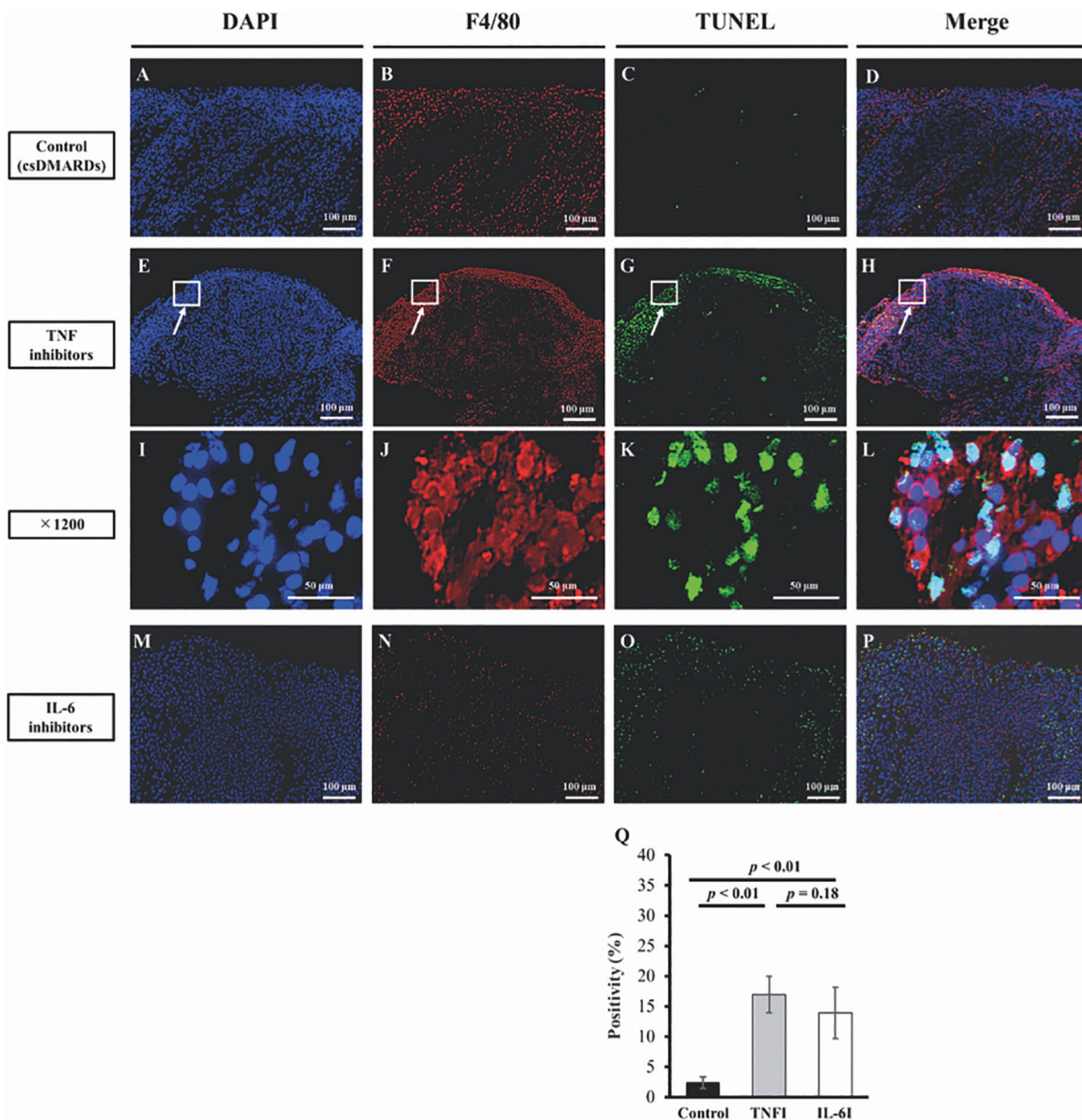


**Fig. 4.** Immunofluorescence staining and score of apoptotic rates in macrophages. **A, B, E, F, M, N:** In all groups, the expression of F4/80 positive cells is widely distributed. **E-F:** In the TNFI group, the F4/80 positive cells are also detected in the lining and sublining layer. **C, G, O, Q:** The sections revealed the positivity of TUNEL-positive cells in the TNFI and IL-6I groups were significantly higher than the positivity of those cells in the control group. **A-P, G:** The TUNEL positive cells appeared especially in the lining and sublining layers of the TNFI group, and the cells were detected as the F4/80 merged cells, which were not observed in the control and IL-6I groups. Kruskal-Wallis test *post-hoc* test for multiple comparisons of samples were used. TUNEL: TdT-mediated non-radioactive fluorescein-deoxyuridine triphosphate nick end labelling; TNFI: TNF inhibitor; IL-6I: IL-6 inhibitor.

were diffusely distributed in the tissue sections of all groups (Fig. 3A-I), with higher expression levels in the control group compared to TNFI and IL-6I groups (Fig. 3D-I). The IH scores for CD86, CD80 (Fig. 2J-K), CD163, and

CD206 (Fig. 3J-K) of the TNFI and IL-6I groups were significantly lower than those of the control group. The immunofluorescence staining of the tissue sections demonstrated that F4/80-positive cells were widely dis-

tributed in control (Fig. 4A-B), TNFI (Fig. 4E-F), and IL-6I groups (Fig. 4M-N), with lower expression levels in the IL-6I group, and higher expression levels in the lining and sublining layer of the TNFI group (Fig. 4E-F).

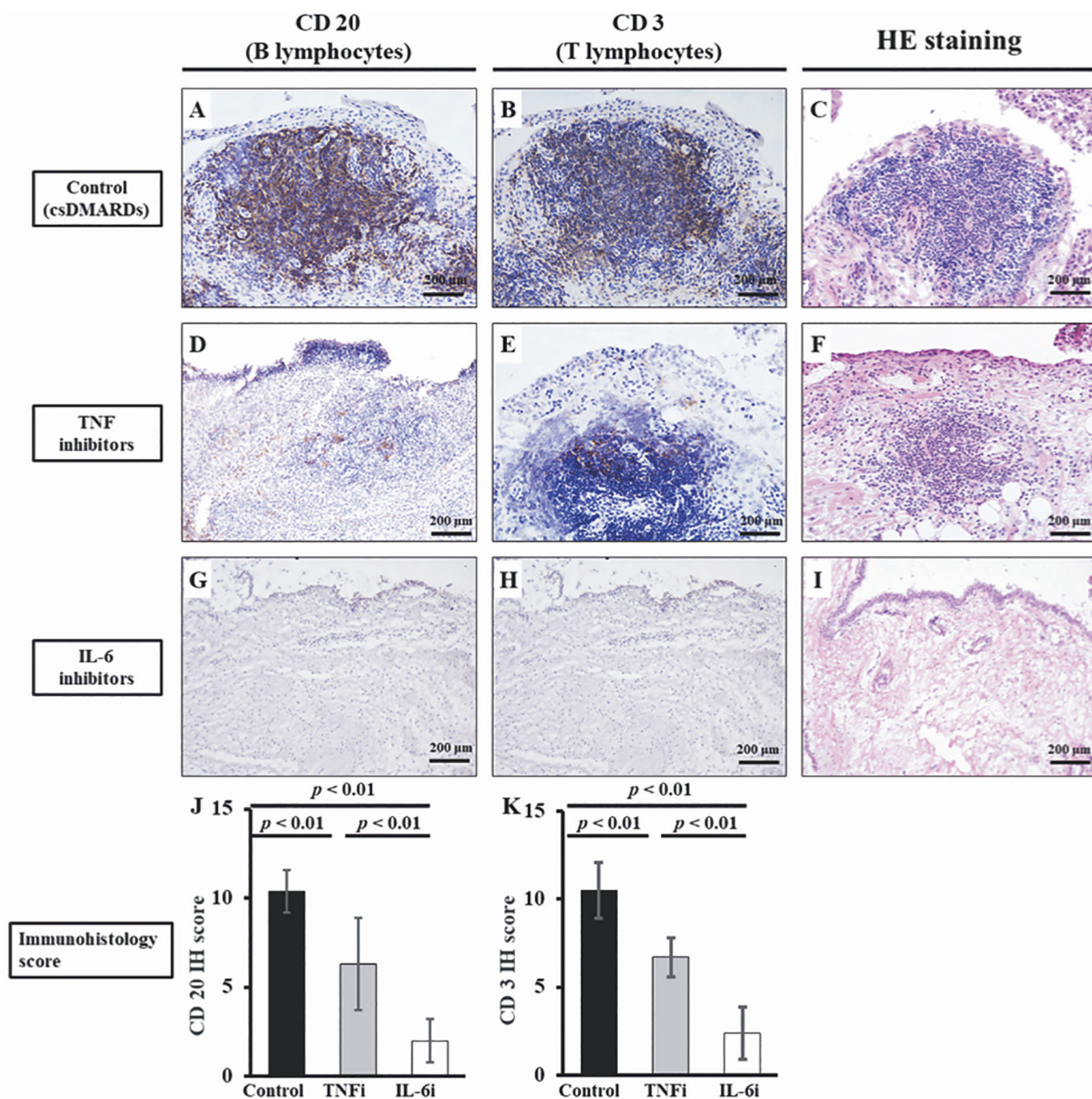


**Fig. 5.** Immunohistochemistry staining and score of CD20 and CD3 for B and T lymphocyte detection in knee joint synovium.

**A-C:** In the control group, the CD20- and CD3-positive cells were detected in sublining layer and surrounding the lymphoid follicle.

**D-F:** In the TNFI group, expression of CD20- and CD3-positive cells is lower compared with that of the control group, particularly in the sublining layer.

**G-I:** In the IL-6I group, expression of CD20- and CD3-positive cells is remarkably lower compared to that in the control group.

**J-K:** The CD20 and CD3 IH scores of the TNFI and IL-6I groups are significantly lower than those of the control group and the scores of the IL-6I group are significantly lower than those of the TNFI group. Kruskal-Wallis test *post-hoc* test for multiple comparisons of samples were used.

CD, cluster of differentiation; TNFI, TNF inhibitor; IL-6I, IL-6 inhibitor.

The results showed that the percentage of TUNEL-positive cells in TNFI and IL-6I groups was significantly higher compared to the control group (Fig. 4C, G, O, Q). In the TNFI group, TUNEL-positive cells were particularly abundant in the lining and sublining layers (Fig. 4G), with TUNEL-

and F4/80-double positive cells being detected (see merged images Fig. 4E-L), while these double-positive cells were not observed in control and IL-6I groups (Fig. 4A-D, M-P).

CD20- and CD3-positive cells were detected in the sublining layer only in the control group (Fig. 5A-I). These cells

were also observed surrounding the lymphoid follicle in the control group (Fig. 5A-C), with the lower expression levels in the TNFI group (Fig. 5D-F), and the lowest expression levels in the IL-6I group (Fig. 5G-I). The quantification of CD20 and CD3 confirmed that IH scores in the TNFI group were sig-

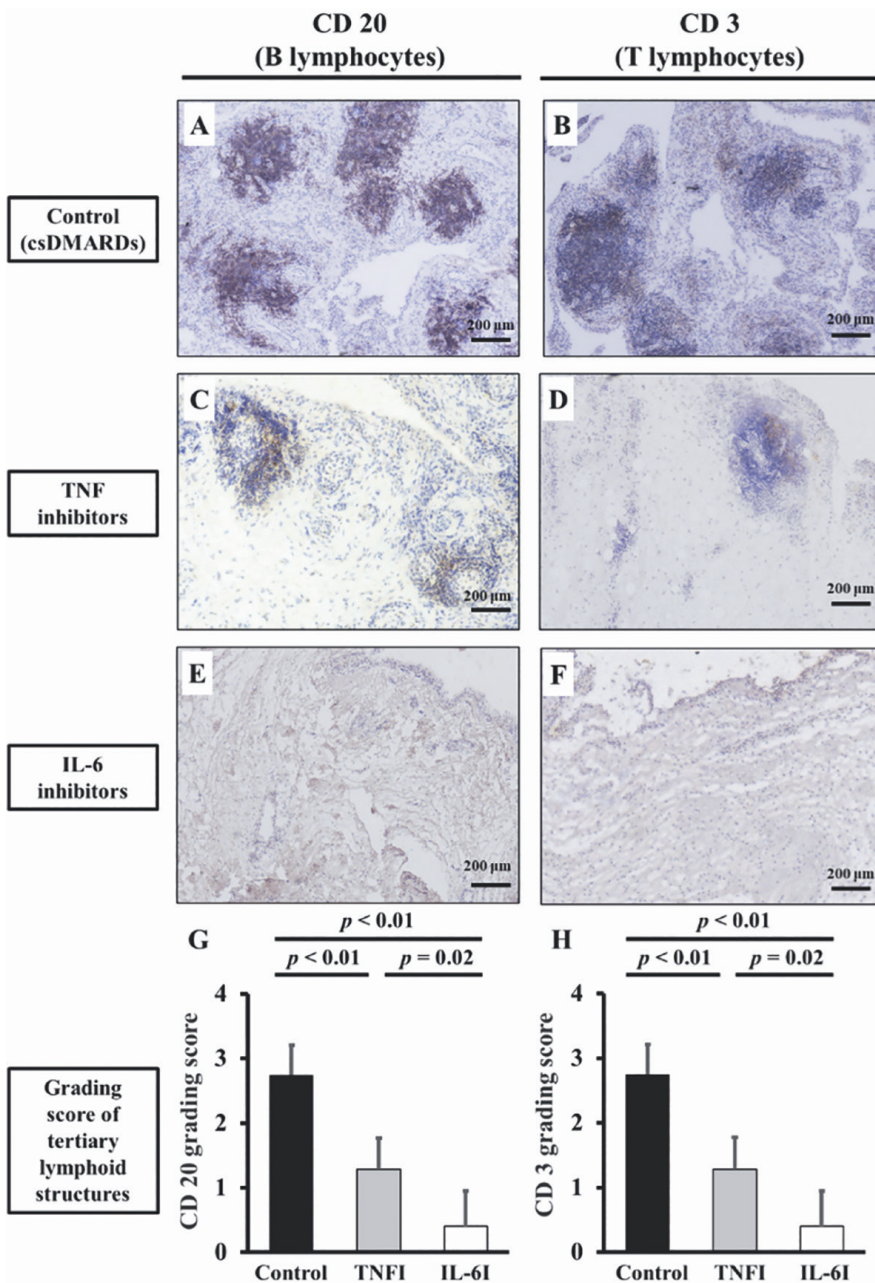


**Fig. 6.** Immunohistochemistry staining and grading score of CD20 and CD3 for tertiary lymphoid structures in knee joint synovium.

A-D, E, F: The TLS were detected in the control group and TNFI group, not detected in the IL-6I group. G-H: The CD20 and CD3 grading score of TLS in the control group were significantly higher than those in the TNFI and IL-6I group, and the scores in the TNFI group were significantly higher than those in the IL-6I groups. Kruskal-Wallis test *post-hoc* test for multiple comparisons of samples were used. TLS: tertiary lymphoid structures; CD: cluster of differentiation; TNFI: TNF inhibitor; IL-6I: IL-6 inhibitor.

nificantly lower than those in the control group, while the scores in the IL-6I group were significantly lower than those in control and TNFI groups (Fig. 5J-K). TLS were detected in control and TNFI groups (Fig. 6A-D), and not detected in the IL-6I group (Fig. 6E-F). The CD20 and CD3 grading scores of TLS in the control group were signifi-

cantly higher than those in TNFI and IL-6I groups, while the scores in the TNFI group were significantly higher than those in the IL-6I group (Fig. 6G-H). The intra-rater interclass correlation coefficient (ICC) and the inter-rater ICC were calculated to examine the reproducibility of measurements. All measurements were performed twice by one

examiner and once by triple-blinded observers. The intra-rater ICCs between two measurements made by the same examiner for IH score of CD86 (Fig. 2J), CD80 (Fig. 2K), CD163 (Fig. 3J), CD206 (Fig. 3K), CD20 (Fig. 5J), CD3 (Fig. 5K), TUNEL positive cell percentage (Fig. 4M), and for grading score of CD20 (Fig. 6G) and CD3 (Fig. 6H) were 0.735, 0.803, 0.788, 0.761, 0.741, 0.931, 0.881, 0.801, and 0.756, respectively. The inter-rater ICCs for IH score of CD86 (Fig. 2J), CD80 (Fig. 2K), CD163 (Fig. 3J), CD206 (Fig. 3K), CD20 (Fig. 5J), CD3 (Fig. 5K), TUNEL positive cell percentage (Fig. 4M), and for grading score of CD20 (Fig. 6G) and CD3 (Fig. 6H) were 0.77, 0.887, 0.939, 0.861, 0.744, 0.805, 0.779, 0.775, and 0.832, respectively.

**Discussion**

Histopathological variations among synovial tissues treated with traditional csDMARDs, TNFIs, and IL-6Is have been previously reported (3, 10-13). However, to the best of our knowledge, our study is the first to investigate the cell types which undergo apoptosis and compare the histological action sites and therapeutic targets of TNFI and IL-6I.

There were no significant variations in average age, disease duration, and serum CRP levels between control groups, the TNFI groups and the IL6I group. DAS28-CRP and treatment regimens – excepting the use of csDMARDs, TNFIs, or IL-6Is – were also comparable among all groups. Although the histopathological features of synovial inflammation have been correlated with disease activity or RA severity (13, 14), our results suggest an additional correlation with the use of TNFIs or IL-6Is. This novel characterisation provides powerful insight into the local immunomodulatory effects of TNFIs and IL-6Is.

The apoptosed cells in the lining and sublining layer of the TNFI-treated tissue chiefly comprised macrophages, uniquely resulting in discoid fibrosis, while those in the deep lining layer of the IL-6I-treated tissue comprised blood vessel-adjacent synovial cells, leading to lymphocytic predominance decline. These distinct outcomes in dis-

tinct locations suggest that the mechanistic and therapeutic targets of TNFI and IL-6I are likely histopathologically dissimilar.

Our investigation of the TNFI group bore results similar to those previously reported, including TNFI-unique discoid fibrosis in the lining layer (11) and a decline in synovial cell count, monocyte and macrophage cell surface markers, and lymphocyte count (22-24). In addition, we detected vacuolation and hydropic degeneration of synovial cells and inflammation suppression via vasculature contraction or obstruction, and obtained significantly lower IH scores than those of the control group. We hypothesised that this suppression of inflammatory cell infiltration and the synovial cell degeneration were a result of TNFI-binding of membrane-associated TNF, which initiates reverse signalling and processes such as apoptosis and cytokine suppression. Furthermore, we identified the pre-discoid fibrosis cells as CD86-, CD80-, CD163-, and CD206-positive and CD20-, CD3-negative, and detected an elevation in TUNEL-positive cells surrounding the discoid fibrosis. The TUNEL positive cells in the lining and sublining layers were significantly increased compared to the control group and TUNEL- and F4/80-double positive cells being detected. The presence of macrophages has previously been detected in the lining layer of the joint synovium (25, 26), and *in vitro* applications of TNFI have resulted in cellularity decline at inflammation sites via induction of monocyte and macrophage apoptosis (27, 28). Apoptotic cells have been directly and indirectly associated with fibrosis (29), suggesting the latter is a result of the former. Therefore, we concluded that the discoid fibrosis resulted from the fibrotic transformation of the apoptosed lining macrophages, which are thus the focal site of TNFI action.

The tissue of the IL-6i group exhibited vasculature contraction or obstruction, apoptosis of synovial cells surrounding blood vessels, and extensive scarring, including perivascular fibrosis in the sublining and deep lining layer. We also detected greater lining layer degeneration with perivascular fibrosis

and a greater decrease in the infiltration of inflammatory cells, especially lymphocytes, in the sublining and deep lining layer than in the TNFI group. IL-6I therapy has been reported to suppress the production of VEGF, a potent angiogenic mediator of IL-6-induced tubule formation in the patient's serum and RA FLS (10, 30). Because TNFI therapy indirectly inhibits VEGF production via IL-6 suppression, IL-6I therapy exhibits a stronger anti-angiogenesis response. Thus, The IL-6I group demonstrated a higher level of TUNEL-positive cells near blood vessels and more pronounced perivascular fibrosis than the TNFI group. Our results also indicated that the IL-6I group exhibited a greater decline of CD86-, CD80-, CD163-, CD206-, CD20-, CD3-positive cells and TLS than the control group, and produced significantly lower CD20 and CD3 IH and grading scores than either the TNFI or the control group. Our observation of a decline in lymphocyte predominance aligned with previous reports of IL-6I therapy suppressing IL-21 production via memory and activated T-cells (31), inhibiting CD4 naïve T cells, CD4 memory T cells, and Th17 cells *in vitro* (32) and reducing memory B-cells (33) We did not observe localisation of macrophage or lymphocyte cells or a remarkable reduction of the former in the IL-6I group. Our evidence suggests the likely IL-6I target is deep lining cells, principally lymphocytes and perivascular cells.

There are some limitations of this study which should be considered. First, the low number of patients involved. More comprehensive studies with larger sample sizes are required to do better statistical analysis. Second, our use of synovial tissue exclusively from knee joints, based on previously reported evidence that inflammation in one joint type is generally representative of that in other joints (34), may present another limitation. Finally, our study did not explore other therapies, such as JAK inhibitors and abatacept, which would potentially provide additional substantiation of our findings.

In summary, the present study clearly demonstrates that TNFIs and IL-6Is target different action sites and synovial

cell types, resulting in histopathological features of synovial tissues that are distinct from one another. We revealed that TNFIs and IL-6Is may suppress RA synovitis by, respectively, inducing apoptosis of synovial lining macrophages and inhibiting lymphoid infiltration and neovascularisation. In addition, this histopathological examination of RA synovium provides context for the exploration of DMARD biological mechanisms in future studies of RA treatment.

### Acknowledgements

We thank Ms Kyoko Tanaka, Ms Mina-ko Nagata, and Ms Maya Yasuda for their technical assistance.

### References

- SCOTT DL, GRINDULIS KA, STRUTHERS GR, COULTON BL, POPERT AJ, BACON PA: Progression of radiological changes in rheumatoid arthritis. *Ann Rheum Dis* 1984; 43: 8-17. <https://doi.org/10.1136/ard.43.1.8>
- ROONEY M, CONDELL D, QUINLAN W *et al.*: Analysis of the histologic variation of synovitis in rheumatoid arthritis. *Arthritis Rheum* 1988; 31: 956-63. <https://doi.org/10.1002/art.1780310803>
- LIPSKY PE, VAN DER HEIJDE DM, ST CLAIR EW *et al.*: Infliximab and methotrexate in the treatment of rheumatoid arthritis. Anti-Tumor Necrosis Factor Trial in Rheumatoid Arthritis with Concomitant Therapy Study Group. *New Engl J Med* 2000; 343: 1594-602. <https://doi.org/10.1056/nejm200011303432202>
- VAN DER HEIJDE D, KLARESKOG L, RODRIGUEZ-VALVERDE V *et al.*: Comparison of etanercept and methotrexate, alone and combined, in the treatment of rheumatoid arthritis: two-year clinical and radiographic results from the TEMPO study, a double-blind, randomized trial. *Arthritis Rheum* 2006; 54: 1063-74. <https://doi.org/10.1002/art.21655>
- NISHIMOTO N, HASHIMOTO J, MIYASAKA N *et al.*: Study of active controlled monotherapy used for rheumatoid arthritis, an IL-6 inhibitor (SAMURAI): evidence of clinical and radiographic benefit from an x ray reader-blinded randomised controlled trial of tocilizumab. *Ann Rheum Dis* 2007; 66: 1162-7. <https://doi.org/10.1136/ard.2006.068064>
- KIM GW, LEE NR, PI RH *et al.*: IL-6 inhibitors for treatment of rheumatoid arthritis: past, present, and future. *Arch Pharm Res* 2015; 38: 575-84. <https://doi.org/10.1007/s12272-015-0569-8>
- FELDMANN M, MAINI RN: Anti-TNF alpha therapy of rheumatoid arthritis: what have we learned? *Ann Rev Immunol* 2001; 19: 163-96. <https://doi.org/10.1146/annurev.immunol.19.1.163>
- KUBOTA A, SUGURO T, NAKAJIMA A, SONOBE M, TSUCHIYA K: Effect of biological agents on synovial tissues from patients with rheumatoid arthritis. *Mod Rheumatol* 2020;

- 30: 282-6. <https://doi.org/10.1080/14397595.2019.1583783>
9. NISHIMOTO N, KISHIMOTO T: Humanized antihuman IL-6 receptor antibody, tocilizumab. *Handb Exp Pharmacol* 2008;151-60. [https://doi.org/10.1007/978-3-540-73259-4\\_7](https://doi.org/10.1007/978-3-540-73259-4_7)
  10. HASHIZUME M, HAYAKAWA N, SUZUKI M, MIHARA M: IL-6/sIL-6R trans-signalling, but not TNF-alpha induced angiogenesis in a HUVEC and synovial cell co-culture system. *Rheumatol Int* 2009; 29: 1449-54. <https://doi.org/10.1007/s00296-009-0885-8>
  11. HIROHATA S, TOMITA T, YOSHIKAWA H, KYOGOKU M: TNF inhibitors induce discoid fibrosis in the sublining layers of the synovium with degeneration of synoviocytes in rheumatoid arthritis. *Rheumatol Int* 2013; 33: 2473-81. <https://doi.org/10.1007/s00296-013-2743-y>
  12. HIROHATA S, ABE A, MURASAWA A, KANAMONO T, TOMITA T, YOSHIKAWA H: Differential effects of IL-6 blockade tocilizumab and TNF inhibitors on angiogenesis in synovial tissues from patients with rheumatoid arthritis. *Mod Rheumatol* 2017; 27: 766-72. <https://doi.org/10.1080/14397595.2016.1259717>
  13. SCHMIDT T, NAJM A, MUSSAWY H *et al.*: General synovitis score and immunologic synovitis score reflect clinical disease activity in patients with advanced stage rheumatoid arthritis. *Sci Rep* 2019; 9: 8448. <https://doi.org/10.1038/s41598-019-44895-9>
  14. YAMANAKA H, GOTO K, MIYAMOTO K: Scoring evaluation for histopathological features of synovium in patients with rheumatoid arthritis during anti-tumor necrosis factor therapy. *Rheumatol Int* 2010; 30: 409-13. <https://doi.org/10.1007/s00296-009-1158-2>
  15. FUNOVITS J, ALETAHA D, BYKERK V *et al.*: The 2010 American College of Rheumatology/European League Against Rheumatism classification criteria for rheumatoid arthritis: methodological report phase I. *Ann Rheum Dis* 2010; 69: 1589-95. <https://doi.org/10.1136/ard.2010.130310>
  16. NEOGI T, ALETAHA D, SILMAN AJ *et al.*: The 2010 American College of Rheumatology/European League Against Rheumatism classification criteria for rheumatoid arthritis: Phase 2 methodological report. *Arthritis Rheum* 2010; 62: 2582-91. <https://doi.org/10.1002/art.27580>
  17. KASAGI N, GOMYO Y, SHIRAI H, TSUJITANI S, ITO H: Apoptotic cell death in human gastric carcinoma: analysis by terminal deoxynucleotidyl transferase-mediated dUTP-biotin nick end labeling. *Jpn J Cancer Res* 1994; 85: 939-45. <https://doi.org/10.1111/j.1349-7006.1994.tb02972.x>
  18. KANBE K, HARA R, CHIBA J, INOUE Y, TAGUCHI M, TANAKA Y: Application of a new immunohistology scoring system (IH score): analysis of TNF- $\alpha$  in synovium related to disease activity score in infliximab-treated patients with rheumatoid arthritis. *Mod Rheumatol* 2014; 24: 910-4. <https://doi.org/10.3109/14397595.2014.887047>
  19. MANZO A, PAOLETTI S, CARULLI M *et al.*: Systematic microanatomical analysis of CXCL13 and CCL21 in situ production and progressive lymphoid organization in rheumatoid synovitis. *Eur J Immunol* 2005; 35: 1347-59. <https://doi.org/10.1002/eji.200425830>
  20. LANDIS JR, KOCH GG: The measurement of observer agreement for categorical data. *Biometrics* 1977; 33: 159-74.
  21. SLABAUGH MA, FRIEL NA, KARAS V, ROMEO AA, VERMA NN, COLE BJ: Interobserver and intraobserver reliability of the Goutallier classification using magnetic resonance imaging: proposal of a simplified classification system to increase reliability. *Am J Sports Med* 2012; 40: 1728-34. <https://doi.org/10.1177/0363546512452714>
  22. TAK PP, TAYLOR PC, BREEDVELD FC *et al.*: Decrease in cellularity and expression of adhesion molecules by anti-tumor necrosis factor alpha monoclonal antibody treatment in patients with rheumatoid arthritis. *Arthritis Rheum* 1996; 39: 1077-81. <https://doi.org/10.1002/art.1780390702>
  23. ERNESTAM S, AF KLINT E, CATRINA AI *et al.*: Synovial expression of IL-15 in rheumatoid arthritis is not influenced by blockade of tumour necrosis factor. *Arthritis Res Ther* 2006; 8: R18. <https://doi.org/10.1186/ar1871>
  24. SMEETS TJ, KRAAN MC, VAN LOON ME, TAK PP: Tumor necrosis factor alpha blockade reduces the synovial cell infiltrate early after initiation of treatment, but apparently not by induction of apoptosis in synovial tissue. *Arthritis Rheum* 2003; 48: 2155-62. <https://doi.org/10.1002/art.11098>
  25. CULEMANN S, GRÜNEBOOM A, NICOLÁS-ÁVILA J *et al.*: Locally renewing resident synovial macrophages provide a protective barrier for the joint. *Nature* 2019; 572: 670-5. <https://doi.org/10.1038/s41586-019-1471-1>
  26. FIRESTEIN GS: Invasive fibroblast-like synoviocytes in rheumatoid arthritis. Passive responders or transformed aggressors? *Arthritis Rheum* 1996; 39: 1781-90. <https://doi.org/10.1002/art.1780391103>
  27. THALAYASINGAM N, ISAACS JD: Anti-TNF therapy. *Best Pract Res Clin Rheumatol* 2011; 25: 549-67. <https://doi.org/10.1016/j.berh.2011.10.004>
  28. MITOMA H, HORIUCHI T, HATTAN *et al.*: Infliximab induces potent anti-inflammatory responses by outside-to-inside signals through transmembrane TNF-alpha. *Gastroenterology* 2005; 128: 376-92. <https://doi.org/10.1053/j.gastro.2004.11.060>
  29. JOHNSON A, DIPIETRO LA: Apoptosis and angiogenesis: an evolving mechanism for fibrosis. *FASEB J* 2013; 27: 3893-901. <https://doi.org/10.1096/fj.12-214189>
  30. GENTILETTI J, FAVA RA: Does vascular endothelial growth factor play a role in interleukin-6 receptor antagonist therapy for rheumatoid arthritis? *Arthritis Rheum* 2003; 48: 1471-4. <https://doi.org/10.1002/art.11043>
  31. CARBONE G, WILSON A, DIEHL SA, BUNN J, COOPER SM, RINCON M: Interleukin-6 receptor blockade selectively reduces IL-21 production by CD4 T cells and IgG4 autoantibodies in rheumatoid arthritis. *Int J Biol Sci* 2013; 9: 279-88. <https://doi.org/10.7150/ijbs.5996>
  32. LI S, WU Z, LI L, LIU X: Interleukin-6 (IL-6) receptor antagonist protects against rheumatoid arthritis. *Med Sci Monit* 2016; 22: 2113-8. <https://doi.org/10.12659/msm.896355>
  33. ROLL P, MUHAMMAD K, SCHUMANN M *et al.*: In vivo effects of the anti-interleukin-6 receptor inhibitor tocilizumab on the B cell compartment. *Arthritis Rheum* 2011; 63: 1255-64. <https://doi.org/10.1002/art.30242>
  34. KRAAN MC, REECE RJ, SMEETS TJ, VEALE DJ, EMERY P, TAK PP: Comparison of synovial tissues from the knee joints and the small joints of rheumatoid arthritis patients: Implications for pathogenesis and evaluation of treatment. *Arthritis Rheum* 2002; 46: 2034-8. <https://doi.org/10.1002/art.10556>